



HAL
open science

Local properties of an AOT monolayer at the oil-water interface: neutron scattering experiments

H. Kellay, T. Hendrikx, J. Meunier, B. Binks, L. Lee

► To cite this version:

H. Kellay, T. Hendrikx, J. Meunier, B. Binks, L. Lee. Local properties of an AOT monolayer at the oil-water interface: neutron scattering experiments. *Journal de Physique II*, 1993, 3 (12), pp.1747-1757. 10.1051/jp2:1993228 . jpa-00247935

HAL Id: jpa-00247935

<https://hal.science/jpa-00247935>

Submitted on 4 Feb 2008

HAL is a multi-disciplinary open access archive for the deposit and dissemination of scientific research documents, whether they are published or not. The documents may come from teaching and research institutions in France or abroad, or from public or private research centers.

L'archive ouverte pluridisciplinaire **HAL**, est destinée au dépôt et à la diffusion de documents scientifiques de niveau recherche, publiés ou non, émanant des établissements d'enseignement et de recherche français ou étrangers, des laboratoires publics ou privés.

Classification

Physics Abstracts

82.70 — 68.10 — 64.10

Local properties of an AOT monolayer at the oil-water interface : neutron scattering experiments

H. Kellay ⁽²⁾, Y. Hendrikx ⁽¹⁾, J. Meunier ⁽²⁾, B. P. Binks ⁽³⁾ and L. T. Lee ⁽⁴⁾

⁽¹⁾ Laboratoire de Physique des Solides (*), Université Paris XI, Bât. 510, 91405 Orsay Cedex, France

⁽²⁾ Laboratoire de Physique Statistique de l'ENS (**), 24 rue Lhomond, 75231 Paris Cedex 05, France

⁽³⁾ School of Chemistry, University of Hull, Hull HU6 7RX, North Humberside, England

⁽⁴⁾ Laboratoire Léon Brillouin (***), C. E. de Saclay, 91191 Gif-sur-Yvette Cedex, France

(Received 27 May 1993, accepted 7 September 1993)

Abstract. — The structures of the AOT-rich phases obtained in mixtures of AOT-alkane-brine at low AOT concentrations and close to the optimal salinity (i.e. the salinity at which the spontaneous curvature of the AOT monolayer is zero) have been investigated by neutron scattering together with a precise study of the phase diagrams. In the case of octane and decane, the phases are lamellar. A detailed study of the local structure of the film shows that for octane, the lamellar phase is constituted of AOT monolayers separated by thick oil and brine films. In the case of decane, it is constituted of AOT bilayers swollen by decane. The thickness of these bilayers has large fluctuations due to fluctuations of the oil film. For dodecane, a succession of three phases was observed with increasing the salinity. At a low salinity it is probably an L_3 phase. As for decane, the film is a bilayer swollen by dodecane. The thickness of the oil film is smaller than that obtained with decane but also exhibits large fluctuations. The other two phases are viscous. At the highest salinity it is probably an oil/brine bicontinuous phase. This difference in phase structure and type correlates well with values of the monolayer bending elastic modulus K and of the saddle-splay modulus \bar{K} .

Introduction.

The properties of an AOT monolayer at the alkane-water interface are strongly dependent on the number N of carbon atoms in the alkane chain. First, the bending elastic modulus K of the monolayer is independent of the salinity ; it is large ($K = 1 k_B T$) for short chain alkanes

(*) Associé au CNRS.

(**) URA 1306 du CNRS, associé aux Universités Paris VI et VII.

(***) Laboratoire mixte CEA-CNRS.

($N < 11$) but small ($K \sim 0.1 k_B T$) for long chain alkanes [1]. Second, the saddle-splay modulus is larger for long chain alkanes than for short chain alkanes [2]. These differences between the properties of the monolayers obtained with short and long alkane chains have been explained by a difference in penetration of the alkane between the tails of the surfactant molecules in the film. The short chain alkanes probably penetrate the AOT monolayer, increase its thickness and its stiffness and consequently its bending elastic modulus, while long chain alkanes, being bad solvents for the surfactant tails, do not penetrate the monolayer. A first test of this hypothesis was the study of the wetting of an AOT monolayer at the brine-air interface [3]. It was found that long chain alkanes ($N > 11$) do not wet this AOT monolayer while a pseudo-partial wetting was observed in the case of short chain alkanes ($6 < N < 11$).

The phase diagrams of AOT-brine-*n*-alkane mixtures are also dependent on the alkane chain length, reflecting the differences in the properties of the monolayer. They were observed before the properties of the AOT monolayers at the alkane-brine interfaces were measured [4]. The most significant differences are observed for low AOT concentrations close to the optimal salinities, which are the salinities at which the spontaneous curvature of the monolayer vanishes (the optimal salinity increases with the alkane chain length). For short alkane chains, the phases rich in AOT are birefringent : they are lamellar phases, while for long alkane chains the phases rich in AOT are not birefringent and are probably bicontinuous phases. These observations are in agreement with the large bending elastic modulus and the negative Gaussian elastic modulus measured on AOT monolayers at oil-brine interfaces when the alkane chain is short, and with small values of the bending elastic modulus and positive values for the Gaussian elastic modulus when the alkane chain is long.

The hypothesis of penetration of the alkanes into the AOT film depending on the length of the alkane chain can be confirmed by a local study of the AOT film : neutron scattering experiments and NMR [5].

In this paper, we present a neutron scattering study of the AOT-rich phases obtained at salinities close to the optimal salinity for octane, decane and dodecane. We have deduced information about the structures of the different phases and about the surfactant film. A precise phase diagram study was required for this work, particularly with dodecane which gives a more complicated phase diagram than the shorter alkanes. Enhanced film contrast in the neutron scattering experiments was obtained using deuterated water, and, in some cases deuterated oil. This allows the observation of the AOT film alone (deuterated oil and water) or the AOT film plus the oil domains (protonated oil and deuterated water). The use of deuterated water in place of regular water has large effects on the extension in salinity of the different phases in the phase diagram and requires a study of the new phase diagram.

Phase diagrams.

A detailed study of the phase diagram of AOT-alkane-brine mixtures has already been carried out by Ghosh and Miller [4]. Our study is limited to the region of the phase diagram where the alkane and the brine are approximately of equal volume initially and the quantity of AOT is low. Corresponding studies of the phase diagram in deuterated water has been made. The phases in equilibrium are obtained by mixing equal volumes of brine and a low concentration solution of AOT in the *n*-alkane (in the following, the salt and the AOT concentrations of a mixture are relative respectively to the brine and the alkane solution and are twice the true concentration in the mixture). The mixtures are studied at 20 ± 0.1 °C. Just after mixing, the mixture is a white and opaque emulsion. This emulsion breaks more or less quickly depending on the salinity giving rise to different phases in equilibrium. At low salinities the emulsion is very stable and, at least for short chain alkanes, does not break in a reasonable time. The succession of phases in equilibrium is very similar to the ones described by Winsor [6] in the

case of microemulsions. At high salinity a water-in-oil microemulsion (droplets of brine surrounded with an AOT film dispersed in a continuous oil phase) is in equilibrium with an excess of brine. It is a Winsor II (WII) equilibrium. At low salinity an aqueous phase rich in AOT is in equilibrium with an excess of oil. We have called this equilibrium Winsor I (WI) but we have not analysed its structure because the study of this part of the phase diagram is very difficult, at least for short chain alkanes. At intermediate salinities, the behaviour is strongly dependent on the length N of the alkane chain. In most cases, a three phase equilibrium is obtained; we call this region of salinities Winsor III (WIII) by analogy with the Winsor III equilibria obtained in the case of bicontinuous microemulsions. However, the phase rich in AOT is not necessarily a microemulsion in these equilibria. The Winsor III region is obtained, as for microemulsions, close to the « optimal » salinity, i.e. when the spontaneous curvature of the AOT monolayer is close to zero.

(i) *Heptane, octane, nonane.* — For $N = 7, 8$ and 9 in the Winsor III region, a lamellar phase is in equilibrium with an excess of brine and an excess of alkane. The lamellar phase is birefringent and incorporates similar quantities of brine and alkane (Fig. 1). It is constituted of monolayers of AOT alternately separated by an alkane and a brine film.

(ii) *Decane.* — A winsor III lamellar phase is also obtained for $N = 10$, but with a different structure. This phase incorporates only a small amount of alkane. Close to the Winsor II (at the highest salinities), it is in equilibrium with an excess of oil and water, but close to the Winsor I (at the lowest salinities) it incorporates all the brine (Fig. 2). The quantity of decane in the lamellar phase at a salinity $S = 0.07$ M is determined by slowly adding small volumes of decane to a solution of AOT (150 mM) in brine (0.07 M of NaCl). Approximately 97 ± 3 cm³ of decane can be added to 1 000 cm³ of AOT solution before an excess oil phase appears. The lamellar phase contains approximately 3.3 molecules of decane per AOT molecule.

(iii) *Undecane-tetradecane.* — For $N = 11-14$, the phase rich in AOT in the Winsor III region is not birefringent and the phase diagram is more complex. It is given for $N = 12$ (Fig. 3) for

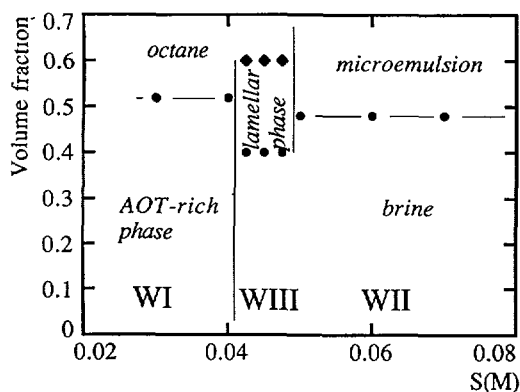


Fig. 1.

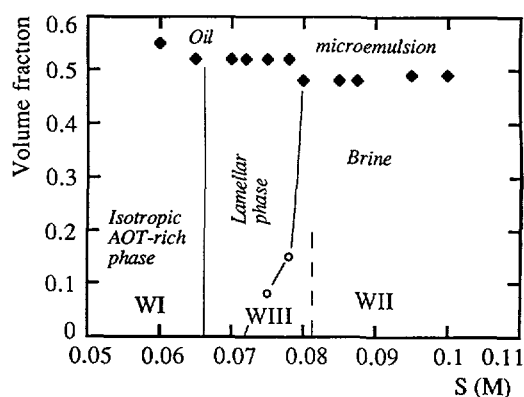


Fig. 2.

Fig. 1. — Volume fraction *versus* the salinity S of the brine for the different phases obtained when equal volumes of protonated brine and a solution of AOT in octane at 30 mM are mixed. $T = 20 \pm 0.1$ °C.

Fig. 2. — Volume fraction *versus* the salinity S of the brine for the different phases obtained when equal volumes of protonated brine and a solution of AOT in decane at 20 mM are mixed. $T = 20 \pm 0.1$ °C.

different AOT concentrations. There are three parts in this Winsor III region. At the Winsor I-Winsor III transition, there is no jump in the volume of the phase rich in AOT. When the salinity increases, the volume of this phase decreases. This is followed by the appearance of two successive jumps in the volume of the AOT-rich phase before the Winsor III-Winsor II transition (these changes can be observed easily at low AOT concentration, Fig. 3a). These discontinuities in the volume *versus* the salinity indicate that the phase rich in AOT is probably a succession of three different phases that we have called B_1 , B_2 and B_3 , respectively. The first one, B_1 , is probably an L_3 phase. Neutron scattering experiments have been performed on two samples of this phase ; one made with deuterated water and protonated alkane, the other with deuterated water and deuterated alkane. The AOT concentration is equal to 15 mM and the salinity $S = 0.13$ M. The results indicate that the scattering objects are flat (Fig. 4), as can be deduced from the slope (at large q) of the plots of the scattered intensity $I(q)$ *versus* q on a log-log scale. This slope is ~ 2 : phase B_1 consists of bilayers of AOT incorporating small amounts of dodecane.

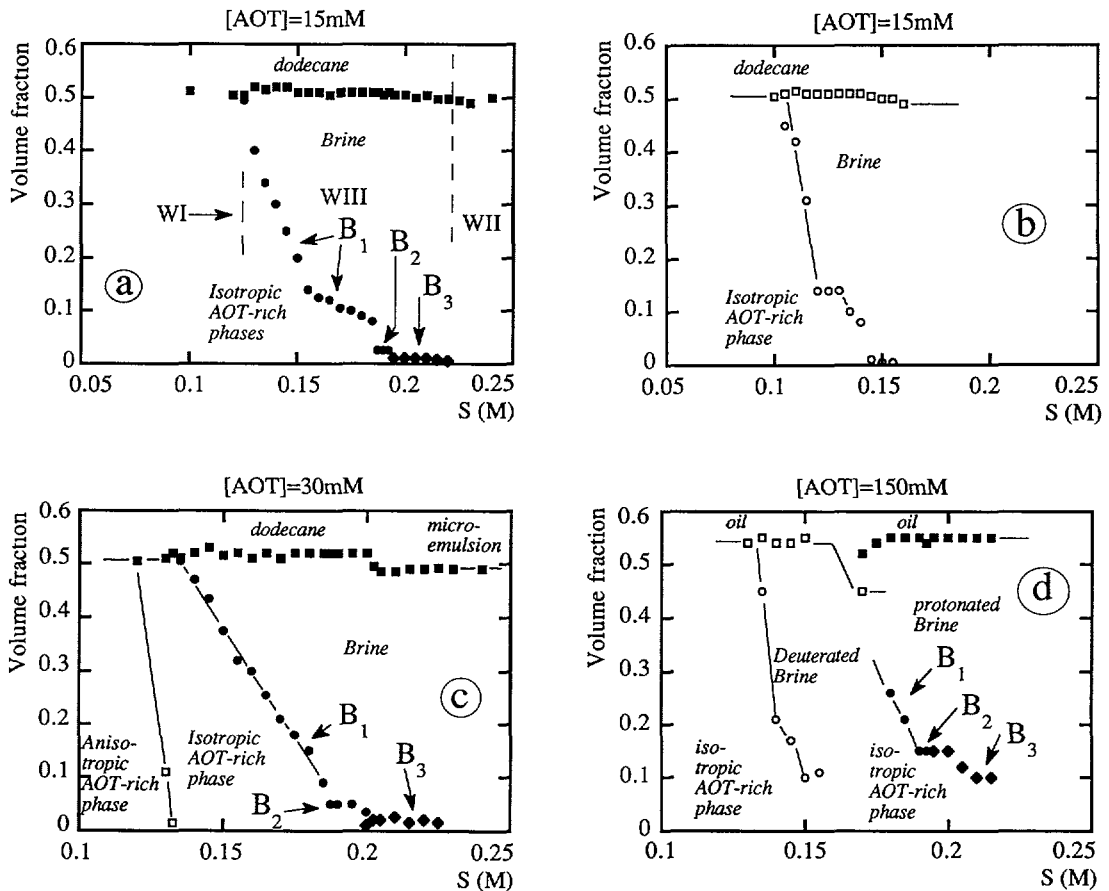


Fig. 3. — Volume fraction *versus* the salinity S of the brine for the different phases obtained when equal volumes of brine and a solution of AOT in dodecane are mixed. a) 15 mM of AOT in the dodecane, protonated water. b) 15 mM of AOT in the dodecane, deuterated water. c) 30 mM of AOT in the dodecane, protonated water. A birefringent phase appears in this phase diagram. d) 150 mM of AOT in the dodecane, (\bullet and \blacksquare) protonated and (\circ and \square) deuterated water. On this last phase diagram the anisotropic phase at low salinity is not represented.

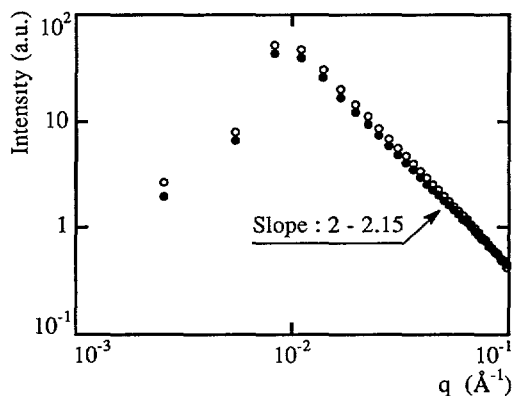


Fig. 4. — Scattered neutron intensity I versus the wave vector q in a log-log scale for the AOT-rich phase (B_1 phase) obtained by adding an excess of protonated (\bullet) or deuterated (\circ) dodecane to a solution of AOT in deuterated brine. The AOT concentration is 15 mM in brine and $S = 0.13$ M. $T = 20$ °C. The slope 2 at large q indicates that the scattering objects are flat.

The two other phases (B_2 and B_3) obtained at higher salinities than the salinities giving phase B_1 are more concentrated in AOT. Their volumes are independent of the salinity and they are viscous. Phase B_3 incorporates more oil than phases B_1 and B_2 but has the smallest volume ; the volume of brine and that of dodecane in this phase are similar. This explains the difference in the density of these two phases. B_2 has a higher density compared to that of brine and appears at the bottom of the vessel, while B_3 has a lower density and appears in the middle of the vessel (between the brine and the oil phases). These phases are obtained in the case of non deuterated water. This density difference allows the observation of a domain of coexistence between phases B_2 and B_3 in a very small range of salinities (Fig. 3) and renders the observation of the phase transition relatively easy. With deuterated water, phases B_2 and B_3 appear in the middle of the vessel (between oil phase and aqueous phase) and their transition with salinity is more difficult to observe. Another difference between phases B_2 and B_3 is that B_2 coexists with an excess of pure alkane (without AOT) while B_3 coexists with an excess of alkane containing a small amount of dissolved surfactant. The oil incorporated in B_1 , B_2 and B_3 phases made with protonated water was determined as before from the oil volume which could be added to an AOT solution (15 mM for B_1 and 150 mM for B_2 and B_3) in brine before saturation. It was found to be 0.8 molecules of dodecane per AOT molecule in the B_2 phase at a salinity $S = 0.19$ M and in the B_1 phase at a salinity $S = 0.13$. In the B_3 phase, at a salinity $S = 0.21$ M, it was found to be 1.2 molecules of oil per AOT molecule.

Neutron scattering experiments performed on a sample of phase B_3 made with both deuterated water and alkane indicate that the scattering objects (AOT monolayer) are flat (dimension 2) while the same experiments performed on a sample made with deuterated water and protonated alkane indicate that the scattering objects (oil + surfactant film) are 3-dimensional one (Fig. 5). The oil domain is not a film in this phase. Phase B_3 is probably a bicontinuous phase in which the oil and the brine domains are separated by an AOT monolayer. Another peculiarity of the B_3 phase is the appearance of an ordered structure with time. The plots of the neutron scattered intensity $I(q)$ versus q on a log-log scale obtained at the LLB a few hours after the cells were filled (Fig. 5a) and the one obtained a few months later at ISIS (Fig. 5b) on the same samples show this evolution. They are similar for the sample made with deuterated water and oil showing only the film. However, the plots obtained with the sample made with protonated dodecane are very different ; a narrow peak appears on the

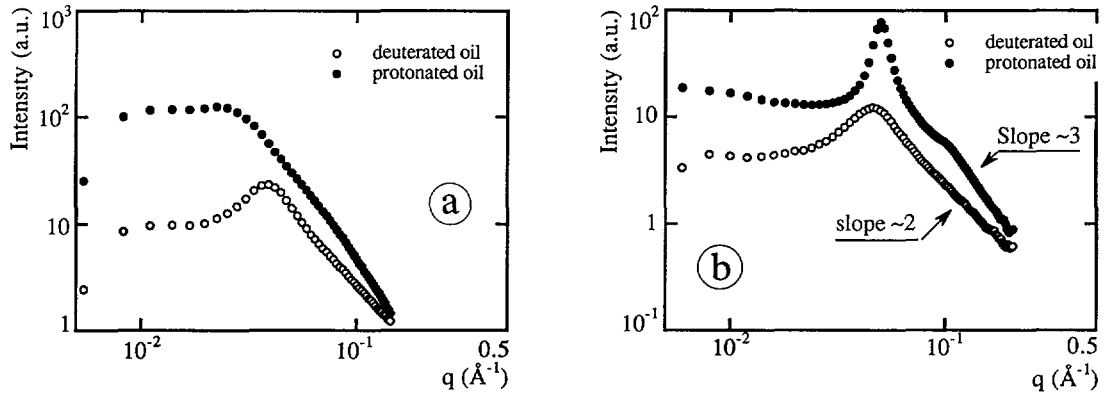


Fig. 5. — Scattered neutron intensity I versus the wave vector q on a log-log scale for the AOT-rich phase (« B_3 » phase) obtained by adding an excess of protonated (●) or deuterated (○) dodecane to a solution of AOT in deuterated brine. The AOT concentration is 150 mM in brine and $S = 0.152$ M. $T = 20 \pm 0.1$ °C. a) spectra obtained a few hours after the cell was filled. b) spectra obtained a few months later. The slopes 2 and 3 at large q indicate that the scattering objects are flat and 3D, respectively.

spectrum obtained at ISIS while no peak is observed on the spectrum obtained at the LLB. No neutron scattering experiment has been performed on the phase B_2 because it is very difficult to extract from a mixture with deuterated water, as explained earlier. On the one hand, the Winsor III region of the phase diagram obtained with deuterated water appears at lower salinities and extend over a smaller range of salinities than with protonated water. On the other hand the two phases B_1 and B_2 obtained in deuterated water, appear in the middle of the tube (between the aqueous phase and the oil phase).

It must be remarked that at low AOT concentration, the Winsor I region is optically isotropic but at a larger concentration, a birefringent phase coexists with the isotropic phase (see Fig. 3c for 30 mM AOT). This phase is not indicated on the phase diagram at 150 mM AOT (Fig. 3d). The quantity of oil incorporated in the birefringent phase is very small, about 0.3 molecules of dodecane per molecule of AOT.

The information obtained with this short study of the phase structures of brine-oil-AOT mixtures at low AOT concentrations and close to the optimal salinities are in agreement with the values of the bending elastic modulus and the saddle-splay modulus measured on an AOT monolayer at the oil-water interface for different alkanes [1, 2]. For short alkane chains, the bending elastic modulus is large ($K \sim k_B T$) and the saddle-splay modulus is negative. The AOT-rich phases are lamellar. For long alkane chains, the bending elastic modulus is small ($\sim 0.1 k_B T$) and the saddle-splay modulus is positive or close to zero. The AOT-rich phase is probably bicontinuous (B_3 phase). These results are in agreement with the theoretical predictions concerning the role of these two moduli [10, 11]. A large K modulus induces a large persistence length $\xi_K \sim \exp(4 \pi K/kT)$ of the monolayer : the surfactant film is flat at a scale of order ξ_K which is large. A negative value for \bar{K} is disfavoured for saddle shapes. In this case lamellar phases are observed. A small K modulus induces a small persistence length of the monolayer : the surfactant film is crumbled by the thermal fluctuations. A positive value for \bar{K} is favourable for saddle shapes. In this case bicontinuous phases are observed.

Film structure.

The neutron scattered intensity $I(q)$ is measured on different samples of the Winsor III region over a large q range. When the slope at high q of the curve $I(q)$ versus q on a log-log plot is

two, the scattering objects are flat, i.e. a surfactant film which is flat at the scale of observation. This film can be a monolayer or a bilayer of AOT incorporating oil, the thickness of which is measured by using two different methods.

At large q , oscillations reflecting the form factor are observed in the plot of $q^4 I(q)$ versus q . For plane layers of thickness d , if $I_c(q)$ is the coherent scattering intensity, the theoretical spectrum is [7]:

$$I_c(q) \sim (1/q^2) [\sin(qd/2)/(qd/2)]^2 = F(q, d).$$

The oscillations are damped because there are fluctuations in the thickness d of the layer. To take this into account, a superposition of functions $F(q, d)$ with different d values was used for the fit:

$$I(q) \sim 2 \times F(q, d) + F(q, d - \Delta d) + F(q, d + \Delta d)$$

where d is the mean thickness of the layer and Δd is related to the mean square amplitude of the fluctuations of the thickness.

At lower q we expect for planar structures [8, 9]:

$$\text{Log}[q^2 I(q)] \sim -d_g q^2/12$$

where d_g is the apparent dry thickness. d_g is deduced from a log-log plot of $q^2 I(q)$ versus q .

The neutron scattering experiments were performed on PAXE at the Laboratoire Léon Brillouin (France) and on LOQ at the Rutherford Appleton Laboratory (England). On PAXE, when the wavelength of the neutron beam is $\lambda = 4.5 \text{ \AA}$ and the distance from the cell to the detector $D \sim 1 \text{ m}$ or 5 m , the q range is $0.02\text{-}0.6 \text{ \AA}^{-1}$ or $0.004\text{-}0.15 \text{ \AA}^{-1}$, respectively. When $\lambda = 13 \text{ \AA}$ and $D \sim 5 \text{ m}$, the q range is $0.001\text{-}0.05 \text{ \AA}^{-1}$. On LOQ, the spectra are obtained with a polychromatic beam and the q range extends from 0.06 to 0.2 \AA^{-1} . The thickness of the samples studied is 1 mm . All the samples are studied at $20 \text{ }^\circ\text{C}$. The control of the temperature is more difficult on PAXE than on LOQ.

The film thickness is deduced from the measurement of the scattered intensity $I(q)$ in samples rich in AOT of the Winsor III domain for octane, decane and dodecane. In each case, the water is deuterated and for decane and dodecane, two samples are studied: one with deuterated alkane in order to observe the AOT monolayer, and the other one with protonated alkane in order to observe the film constituted of an oil film and two AOT monolayers. For octane, only a sample made with deuterated water and oil has been studied because the oil film is too thick to be observed by neutron scattering. First, d and Δd are deduced from the fit of the experimental values of Iq^4 at large q with the theoretical curve $I_c(q)q^4$. In fact, the experimental values I are the sum of the coherent and the incoherent scattering. The measurement of the incoherent scattering I_{inc} to a good accuracy is difficult but it is independent of q . A better accuracy is obtained if I_{inc} is used as a parameter of the fit in addition to d and Δd (3 parameters). The best fits are given in figure 6 for octane ($[\text{AOT}] = 150 \text{ mM}$, $S = 0.03 \text{ M}$), figure 7a for deuterated and figure 7b for protonated decane ($[\text{AOT}] = 30 \text{ mM}$, $S = 0.05 \text{ M}$) and figure 8a deuterated and figure 8b for protonated dodecane ($[\text{AOT}] = 15 \text{ mM}$, $S = 0.13 \text{ M}$, phase B₁).

In a second step, a second value for the film thickness is deduced from the slope of the straight line obtained by plotting $\ln [(I - I_{\text{inc}}) q^2]$ versus q^2 for values of q smaller than before (Figs. 9-11). In this plot the value I_{inc} for the incoherent scattered intensity is that deduced from the previous fit. The thicknesses of the scattering films in the different phases studied obtained by the two methods are given in table 1. The two methods give similar values, the maximum difference between the thicknesses d and d_g obtained from the two methods is 1.5 \AA . In one

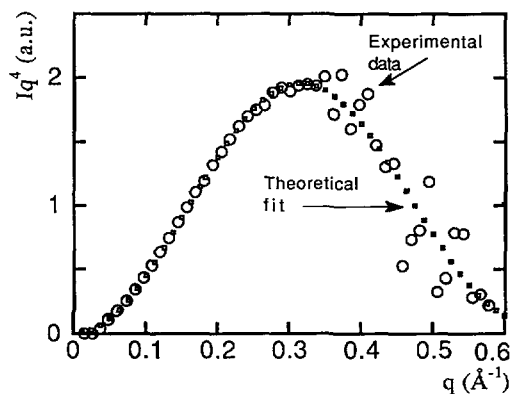


Fig. 6. — Iq^4 versus q at large q for a sample of lamellar phase of AOT-octane-brine obtained by adding an excess of deuterated octane to a solution of AOT in deuterated brine. [AOT] = 150 mM, $S = 0.03$ M. Circles : experimental spectrum, squares : theoretical spectrum.

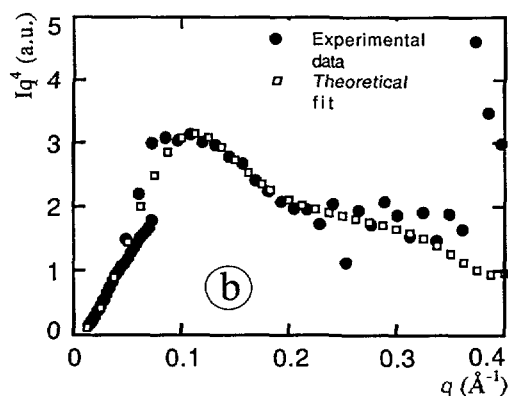
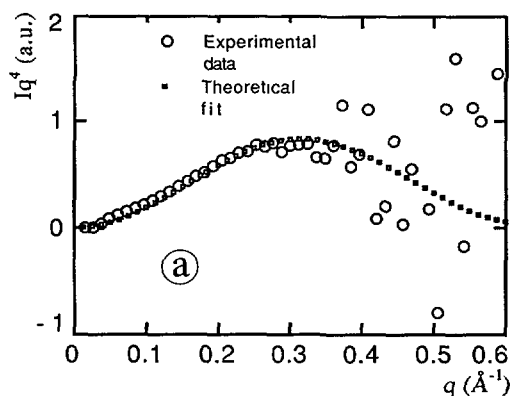


Fig. 7. — Iq^4 versus q at large q for samples of lamellar phase of AOT-decane-brine obtained by adding an excess of a) deuterated decane b) protonated decane to a solution of AOT in deuterated brine. [AOT] = 30 mM, $S = 0.05$ M. Circles : experimental spectrum, squares : theoretical spectrum.

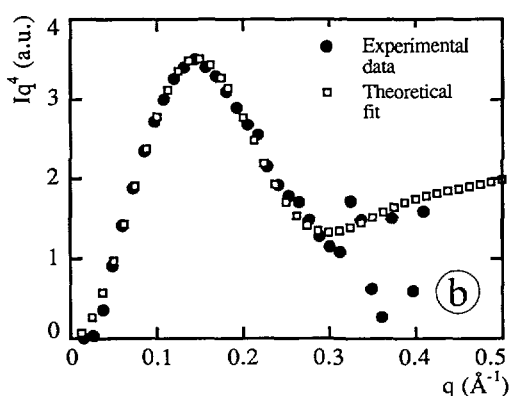
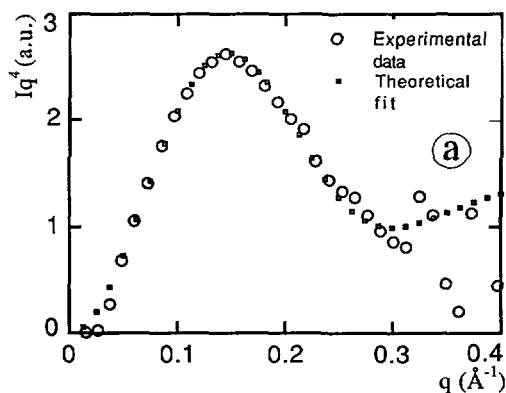


Fig. 8. — Iq^4 versus q at large q for samples of L_3 phase (B_1 phase) of AOT-decane-brine obtained by adding an excess of a) deuterated dodecane b) protonated dodecane to a solution of AOT in deuterated brine. [AOT] = 15 mM, $S = 0.13$ M. Circles : experimental spectrum, squares : theoretical spectrum.

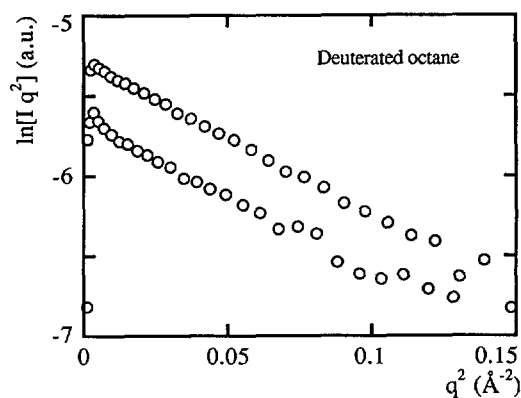


Fig. 9. — Iq^2 versus q^2 on a semi-logarithmic scale in the intermediate q range. Same sample as that of figure 6 (the two curves have been obtained on two different runs).

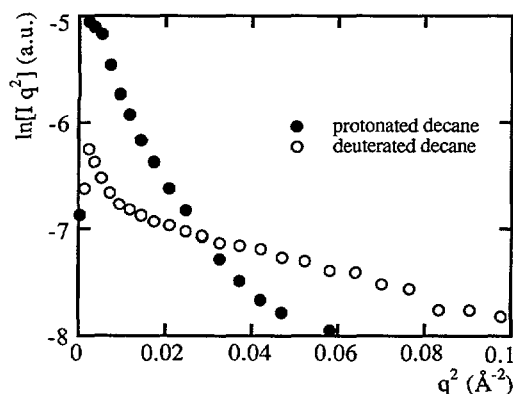


Fig. 10.

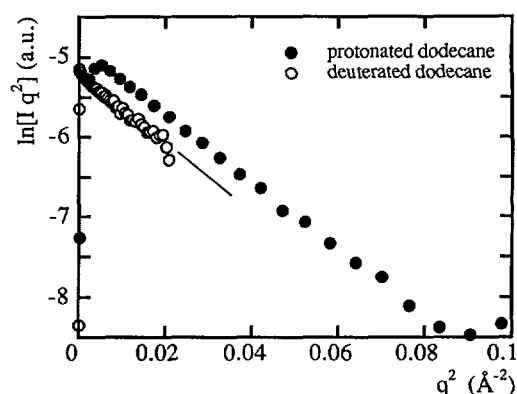


Fig. 11.

Fig. 10. — Iq^2 versus q^2 on a semi-logarithmic scale in the intermediate q range. Same sample as those of figure 7. (○) deuterated decane, (●) protonated decane.

Fig. 11. — Iq^2 versus q^2 on a semi-logarithmic scale in the intermediate q range. Same sample as those of figure 8. (○) deuterated dodecane, (●) protonated dodecane.

case (protonated decane) the plot $\ln(Iq^2)$ versus q^2 is not possible; the experimental points are not on a straight line. We think that this results from a precipitation of the phase studied during the experiment, due to an inadequate thermostating. A rough estimation of d_g in this case gives 26 Å, a value significantly different from the 31 Å obtained by the first method.

When both the oil and water are deuterated and the oil film is thicker than the wavelength of the neutron beam, the measured thickness is that of the AOT monolayer. This is the case with octane and decane and the thickness is $d \approx 10$ Å. The fluctuations of the thickness of this monolayer are small ($\Delta d \sim 1$ Å). In both cases, d_g is larger than but close to d . With protonated oils the film observed by neutron scattering is the bilayer of AOT swollen with oil (Fig. 12). It has been measured only with decane and dodecane. With octane, the thickness of the oil film is too large to be measured. It must be remarked that the fluctuations of the thickness of the

Table I. — Thickness of the surfactant film deduced from the plot of Iq^4 versus q and that of $\log(Iq^2)$ versus q^2 for the different samples. It is not possible to measure d_g on the sample with the protonated decane. This is due to an inadequate temperature regulation on PAXE.

	Deuterated octane	Deuterated decane	Protonated decane	Deuterated dodecane B ₁ phase	Protonated dodecane B ₁ phase
Iq^4	$d = 10 \text{ \AA}$ $\Delta d = 1 \text{ \AA}$	$d = 10 \text{ \AA}$ $\Delta d = 1 \text{ \AA}$	$d = 31 \text{ \AA}$ $\Delta d = 12 \text{ \AA}$	$d = 22.5 \text{ \AA}$ $\Delta d = 6.5 \text{ \AA}$	$d = 21 \text{ \AA}$ $\Delta d = 5 \text{ \AA}$
Iq^2	$d_g = 10.85 \text{ \AA}$	$d_g = 11.4 \text{ \AA}$		$d = 22.5 \pm 1 \text{ \AA}$	$d = 22.5 \text{ \AA}$

DEUTERATED BRINE

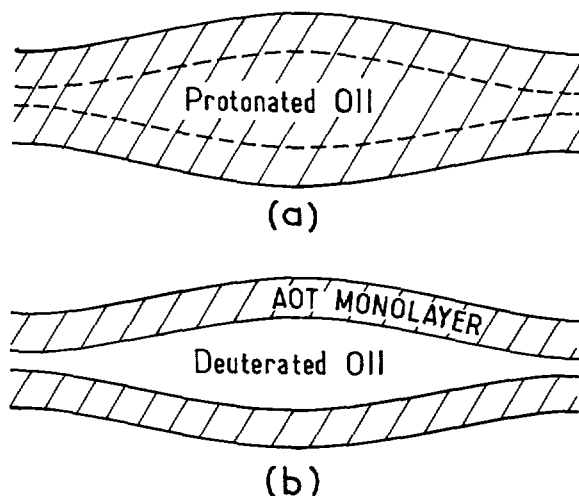


Fig. 12. — Schematic structure of the film observed in a neutron scattering experiment depending on whether the alkane is a) protonated b) deuterated.

swollen bilayers are large ($\sim 12 \text{ \AA}$ for a bilayer thickness of $\sim 31 \text{ \AA}$ and $\sim 5 \text{ \AA}$ for a bilayer thickness of $\sim 22 \text{ \AA}$, with decane and dodecane respectively). They are larger than twice those of the monolayer. The thickness of the incorporated oil film fluctuates approximately between 0 and 6 \AA for dodecane, and between 0 and 20 \AA for decane (Fig. 12). In the case of the sample with deuterated dodecane, the measured thickness is the same as with protonated dodecane, i.e. that of the bilayer. In this case the deuterated oil film is not observed because its thickness is smaller than the wavelength of the neutron beam used for these experiments (4.5 \AA). It is not possible to measure the thickness of the monolayer at the dodecane-brine interface.

Conclusions.

The results presented on the phase structures of brine-oil-AOT mixtures at low AOT concentrations and close to the optimal salinities are in agreement with the values of the bending elastic modulus and the saddle-splay modulus measured on an AOT monolayer at the oil-water interface for different alkanes [1, 2]. For short alkane chains, the bending elastic modulus is large ($K \sim k_B T$) and the saddle-splay modulus is negative, and the AOT-rich phases are lamellar. For long alkane chains, the bending elastic modulus is small ($\sim 0.1 k_B T$) and the saddle-splay modulus is positive or close to zero, and the AOT-rich phase is probably bicontinuous (B_3 phase). These results agree with the theoretical predictions on the role of these two moduli [10, 11]. The lamellar phase with decane and the L_3 phase with dodecane are constituted of bilayers having incorporated alkane. Large thermal fluctuations are observed in the thickness of the alkane film between the two AOT-monolayers. The thickness of the alkane film, which increases with decreasing alkane chain length, is controlled by entropic forces together with van der Waals forces and the short range forces as in the case of an oil film at the AOT-air interface [3].

Acknowledgments.

The authors wish to thank J. Teixeira and R. Heenan for their assistance on Paxe and LOQ.

References

- [1] Binks B. P., Kellay H. and Meunier J., *Europhys. Lett* **16** (1991) 53.
- [2] Kellay H., Meunier J. and Binks B. P., *Phys. Rev. Lett.* **70** (1993) 1485.
- [3] Kellay H., Meunier J. and Binks B. P., *Phys. Rev. Lett.* **69** (1992) 1220.
- [4] Ghosh O. and Miller C. A., *J. Phys. Chem.* **91** (1987) 4528.
- [5] Hendrikx Y., Kellay H. and Meunier J., submitted to *Europhys. Lett*
- [6] Winsor P. A., *Solvent Properties of Amphiphilic Compounds* (Butterworths, London, 1954).
- [7] Marignan J., Apell J., Bassereau P., Porte G. and May R. P., *J. Phys. France* **50** (1989) 3553.
- [8] Guinier A. and Fournet G., *Small angle Scattering of X-rays* (Wiley, N.Y., 1955).
- [9] Cabane B., Duplessix R. and Zemb T., *J. Phys. France* **46** (1985) 2161 ;
Cabane B., *Surfactant solutions, new methods of investigation*, R. Zana Ed. (Marcel Dekker, N.Y., 1987) p. 57.
- [10] de Gennes P. G. and Taupin C., *J. Phys. Chem.* **86** (1982) 2294.
- [11] Porte G., Apell J., Bassereau P. and Marignan J., *J. Phys. France* **50** (1989) 1335.